Optimal design of stiffened plate subjected to combined stochastic loads

Y. Garbatov
Centre for Marine Technology and Ocean Engineering (CENTEC), Instituto Superior Técnico, Universidade de Lisboa, Lisbon, Portugal

P. Georgiev
Technical University of Varna, 1, Studentska Str. UPB, 201, Varna, Bulgaria

ABSTRACT: The objective of this work is to perform a multi objective nonlinear structural optimization of a stiffened plate subjected to combined stochastic compressive loads accounting for the ultimate strength and reliability based constraints in the design. The solution of a dual objective structural response, in minimizing the weight and structural displacement, is considered as a multi-objective optimization problem. The Pareto frontier solution is used to define the feasible surface of the design variables. The reliability index, which defines the shortest distance from the origin to the limit-state boundary, is employed to identify the topology of the stiffened plate as a part of the Pareto frontier solution in reducing the failure probability for the critical limit states by satisfying the target reliability level and identifying the existence of risk driven by the design solution.

1 INTRODUCTION

Steel stiffened plates are predominantly used in ship structural design. The recent development in structural reliability methods and optimisation tools permits a coupled reliability based design approach to be employed in which the uncertainties related to the design variables can be directly accounted for.

The reliability analysis explored here is using the first order reliability methods, FORM that provide a way of evaluating the reliability efficiently with a reasonably good accuracy, which is adequate for practical applications as provided by Rackwitz and Fiessler (1978) and Ditlevsen (1979).

Predominantly FORM approaches have been used for a structural assessment as shown by Garbatov and Guedes Soares (2008, 2011), but may also be employed for a probabilistic analysis of the survival index after ship flooding. as demonstrated by Georgiev and Naydenov (2015).

A genetic algorithm with a termination criteria is employed here (Deb et al., 2002, Wong et al., 2015) for a non-linear optimization problem in defining the best design solutions of the stiffened plate subjected to compressive loads. The genetic algorithm of (Deb et al., 2002) accommodates fast non-dominated sorting procedure, implementing an elitism for the multi-objective search, using an elitism preserving advanced approach allowing both continuous and discrete design variables.

Pareto frontier (Komuro et al., 2006) is applied for a simultaneous minimization of the net sectional area and structural displacement.

Employing the Pareto Frontier, an optimal solution accounting for the existing constraints may be chosen using a utility function to rank the different designs, or by using 2D or 3D scatter diagrams to identify the more attractive ones. In the present case study, an additional constraint is introduced representing the target reliability level to choose the most appropriate design solution.

A three-step approach for design of stiffened plate is presented that couples the reliability methods and structural optimization techniques. Once the structural topology is defined, the scantling of the structural components of the stiffened plate is performed and optimized, in which the design variables, objective functions related to the minimum net sectional area, which leads to a minimum weight and minimum displacement and constraints, including the ultimate compressive strength are defined in a purely deterministic manner. Then the Pareto frontier is used to define the most suitable design solutions in minimizing both objective functions, satisfying all constraints. The design solutions at the Pareto frontier is then used as a basis for the reliability-based optimization regarding the target reliability level that is required to guarantee the structural integrity in which the limit state function is composed by the selected stochastically described design variables. This step accommodates the uncertainties related to the design variables and involved computational models.

The objective here is to perform a multi objective, nonlinear structural optimization of a stiffened plate subjected to combined stochastic compressive loads accounting for the ultimate strength and reliability based constraints in the design. The Pareto frontier, ultimate limit state and target reliability, defined as additional constraints are employed to identify the

optimal design solution. Sensitivity of the design and random parameters are analysed and the partial safety factor that can be used in an early stage of design are defined.

2 STRENGHT ASSESSMENT

2.1 Structural description

Longitudinal stiffened plate of an angular profile is used to build a bottom structure of a tanker ship is analysed in the present study (see Figure 1). The principal dimensions of the tanker are: the length between the perpendiculars, L=139.5 m, depth, D =12.4, breadth, B=21.6 m, draft, d =10.0 m, DW=15000 tons, block coefficient, C_b=0.75. The still water bending moment in hogging and sagging are given according to IACS (2012), $M_{sw,h}^{CSR}$=407616.4 kNm, $M_{sw,s}^{CSR}$=-345328.99 kNm and the wave-induced moments $M_{w,h}^{CSR}$= 522115.4 kNm and $M_{w,s}^{CSR}$=-584402.9 kNm respectively.
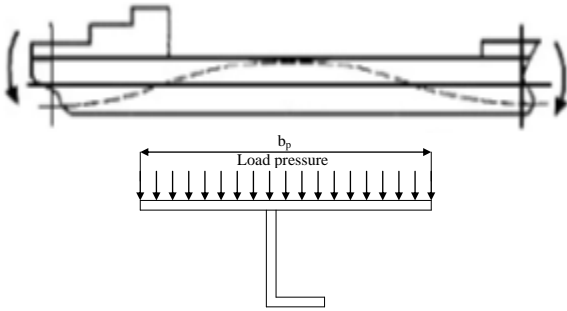

Figure 1 Global (up) and local (down) loads

The local static and dynamic pressure loads are given as P_{sw}^{CSR}=88 kPa and P_w^{CSR}=13 kPa. The inertia moment of the midship net section with respect to the neutral axis is I_{na} = 83.53 m^4 and the midship section modulus with respect to the bottom line is W_b = 5.88 m^3. The yield strength is σ_y=315 MPa and the Young modulus is E=210 GPa.
The span of the longitudinal stiffener (stiffened plate) is l=2.4 m. The distance between the longitudinal stiffeners is b_p=0.8 m. The rest of the parameters as can be seen from
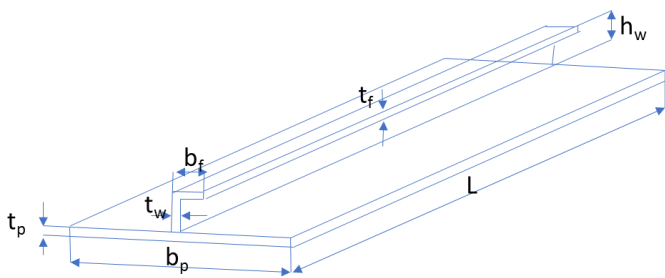Figure 2 are defined during the optimization process.

Figure 2 Stiffened plate

2.2 Structural load

The studied longitudinal stiffener is subjected to axial stresses resulting from the vertical still water and wave-induced bending moments, σ_{global}= (M$_{sw}$+ψM$_{sw}$)/W$_{bottom\ ship}$, where ψ is a combination factor between the still water and wave induced loads ranging from 0.8 to 0.95 depending on the assumptions (Guedes Soares, 1992, Wang and Moan, 1996) and it is assumed here to be a deterministic one of 0.9.The stiffener plate is also subjected to a lateral load, induced by the hydrostatic and dynamic local pressure, q_{local}=(P$_{sw}$+ψP$_w$)b$_p$.

The stiffened plate is assumed to be a simply supported beam subjected to a uniformly distributed lateral load, q_{local} and axial tensile force T=A(M$_{sw,s}$+ψM$_{w,s}$)/W$_{bottom\ ship}$ in the case of sagging loading and to an axial compressive force T*= A (M$_{sw,h}$+ψM$_{w,h}$)/W$_{bottom\ ship}$ in the case of hogging respectively, where A is the net sectional area of the stiffened plate. In the present study, only the compressive load will be considered in the design of the stiffened plate.

The differential equation of a simply supported beam subjected to a uniformly distributed lateral load, q_{local} and an axial force, T can be presented as (Shimansky, 1956, Timoshenko and Gere, 1986):

$$EIz^{IV} - Tz'' = q(x) \tag{1}$$

where the solution of the differential equation can be defined as:

$$z = z_{gs} + z_{ps} \tag{2}$$

The general solution of the differential equation with respect to the displacement, z_{gs} is given by:

$$z_{gs} = A_1 + A_2 kx + A_3 ch(kx) + A_4 sh(kx) \tag{3}$$

and the particular solution, z_{ps} is defined as:

$$z_{ps} = -\frac{qx^2}{2T} \tag{4}$$

The origin of the assumed coordinate system is located at the middle of the span of the stiffened plate. Since the elastic line of the beam is symmetrical with respect to the middle of the span of the stiffened plate A_2=A_4=0 and

$$z(x) = -\frac{qx^2}{2T} + A_1 + A_3 ch(kx) \tag{5}$$

The coefficients A_1 and A_3 are defined taking into account the boundary conditions at the supports:

$$x = \pm\frac{l}{2} \begin{cases} z = 0 \\ z'' = 0 \end{cases} \tag{6}$$

resulting in a system of equations:

$$\left| \begin{aligned} A_1 + A_2 ch\left(\frac{kl}{2}\right) &= \frac{ql^2}{8EIk^2} \\ A_3 k^2 ch\left(\frac{kl}{2}\right) &= \frac{ql^2}{EIk^2} \end{aligned} \right. \tag{7}$$

that defines the coefficients A_1 and A_3 as

$$A_1 = \frac{q}{EIk^4}\left[\frac{k^2l^2}{8}-1\right] \text{ and } A_3 = \frac{q}{EIk^4}\frac{1}{ch\left(\frac{kl}{2}\right)} \quad (8)$$

Substituting A_1 and A_3 in the general solution, and taking that into account:

$$u = \frac{kl}{2} = \frac{l}{2}\sqrt{\frac{T}{EI}} = \frac{l}{2}\sqrt{\frac{\sigma_{global}A}{EI}} \quad (9)$$

in the case of a compressive axial force load, $T^*=T<0$, the maximum displacement and bending moment at $x=0$ are defined as:

$$z_{x=0}\left(u^*\right) = -\frac{5}{384}\frac{ql^4}{EI}f_o^*\left(u^*\right) \quad (10)$$

$$m_{x=0}\left(u^*\right) = \frac{ql^2}{8}\phi_o^*\left(u^*\right) \quad (11)$$

where the magnification functions, $f_o^*(u^*)$ and $\phi_o^*(u^*)$ with respect to the displacement, $z_{x=0}(u^*)$ and bending moment, $m_{x=0}(u^*)$, in the case $T^*<0$, are given as:

$$f_o^*\left(u^*\right) = \frac{24}{5(u^*)^4}\left(\frac{1}{\cos(u^*)}-\frac{(u^*)^2}{2}-1\right) \quad (12)$$

$$\phi_o^*\left(u^*\right) = \frac{2}{(u^*)^2}\left(\frac{1}{\cos(u^*)}-1\right) \quad (13)$$

where:

$$u^* = \frac{kl}{2} = \frac{l}{2}\sqrt{\frac{T^*}{EI}} \text{ and, } T^* = \frac{\pi^2 EI}{l^2} \quad (14)$$

In the case when $u^*=\pi/2$ buckling failure occurs since $f_o^*(u^*)=\phi_o^*(u^*)=\infty$.

The maximum stresses at the middle of the beam are calculated as:

$$\sigma_{max,x=0} = \sigma_{local}+\sigma_{global} \quad (15)$$

where

$$\sigma_{local}\left(P_{sw},P_w\right) = \frac{m_{x=0}\left(u^*\right)}{W_{stiffened\ plate}} \quad (16)$$

$$\sigma_{global}\left(M_{sw,s},M_{w,s}\right) = \frac{M_{sw,s}+\psi M_{w,s}}{W_{bottom\ ship}} \quad (17)$$

However, due to the local outside water pressure load that is subjected to the bottom plate of the ship, the bottom line of the stiffened plate is subjected to axial compressive stresses as calculated by Eqn (16).

2.3 *Structural capacity*

The structural integrity of structures can be analysed, in the case of tensile load based on the permissible stresses that are as a function of yield stresses of the material (Figure 3) and on buckling or ultimate strength in the case of compressive loading (Figure 4). In both cases the stress-strain material property relationship is fundamental (Garbatov et al., 2016a).

For the ultimate strength assessment, an idealized stress-strain or load-displacement relation may be used (see Figure 4). The ultimate limit state of structures represents the collapse because of the loss of stiffness and strength. It relates to the loss of the equilibrium in a party or to the entire structure from buckling and plastic collapse of plating, stiffened panels and supporting members.
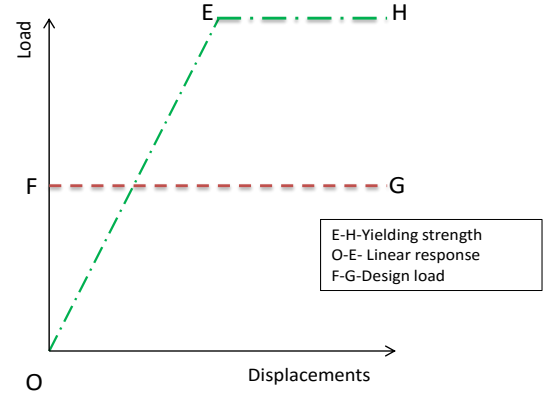

Figure 3 Material load-displacement relationship (tensile load)

The elastic buckling strength in the elasto-plastic relationships is represented by point B and the ultimate strength by point C as shown in Figure 4 (Garbatov et al., 2016a).

The safety margin of structures can be evaluated by a comparison of the ultimate strength with the extreme applied (design) loads, line FG as shows in Figure 4. The structural assessment may be performed to assess the ultimate strength and the damage tolerance and survivability.

It has to be pointed out that the ultimate strength reduction is governed by many factors such as the initial imperfection (Tekgoz et al., 2012), boundary conditions and load effect (Garbatov et al., 2011), corrosion plate surface roughness (Silva et al., 2013), residual stresses (Tekgoz et al., 2013a, b, 2014) and material properties change (Garbatov et al., 2014) due to the corrosion degradation and have an adverse effect on the ultimate strength.
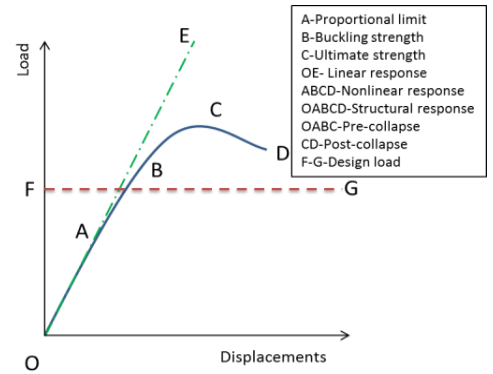

Figure 4 Load-displacement relationship (compressive load)

An algorithm, based on the stipulated by IACS (2012), a simplified method based on an incremental-iterative approach procedure for estimating the elasto-plastic failure of the stiffened plate, σ_u leading to a beam

column and web local buckling of the stiffened plate, is employed here (Garbatov et al., 2016b). The algorithm estimates the stress –strain relationship and ultimate load capacity, σ_u.

3 STRUCTURAL OPTIMIZATION

A genetic algorithm with a termination criteria is employed here defined as a non-dominated sorting generic algorithm, NSGA-II developed by Deb et al. (2002) in defining the best design solutions of the stiffened plate subjected to compressive loading. The objective functions and the constraints, involving the design variables, are nonlinear resulting in a non-linear optimization problem.

Five steps in the genetic algorithm are followed including, 1 - generation of initial population, 2 -sorting the population based on the Pareto non-domination criteria, 3 - evaluation of any individual fitness according to the Pareto ranking, 4 - parent selection based on the individual fitness, 5 - application of genetic operators to generate new population, 6 - identifying the best non-dominated solution and finally, 7 - verifying the convergence and found ends the process otherwise return to step 3.

The genetic algorithm NSGA-II stops when it cannot accommodate into a non-dominated solution set.

3.1 Decision Variables

The decision variables assumed here are $x_1 = t_p$, $x_2 = b_f$, $x_3 = t_f$, $x_4 = h_w$, $x_5 = t_w$, $\mathbf{x} = \{ x_1, x_2, x_3, x_4, x_5 \}^{-1}$ (see Figure 2) and their range is defined as:

$$x_{i,min} \leq x_i \leq x_{i,max} , \ i \in [1,5] \quad (18)$$

where:

$$x_{1,min} = t_{min}, \ x_{1,max} = t_{max} \quad (19)$$

$$x_{2,min} = 0.25 h_{min}, \ x_{2,max} = 0.25 h_{max} \quad (20)$$

$$x_{3,min} = t_{min}, \ x_{3,max} = t_{max} \quad (21)$$

$$x_{4,min} = h_{min}, \ x_{4,max} = h_{max} \quad (22)$$

$$x_{5,min} = t_{min}, \ x_{5,max} = t_{max} \quad (23)$$

where $t_{min}=0.004m$, $t_{max}=0.025m$, $h_{min} =0.1m$ and $h_{max}=0.25m$.

3.2 Objective functions

The dual objective structural response considered here is minimizing the weight, which leads to minimizing of the net sectional area and minimizing the structural displacement, which defines a multi-objective optimization problem:

$$F_1=min \ \{z_{x=0}(\mathbf{b}, \mathbf{x})\} \quad (24)$$
$$F_2=min \ \{A(\mathbf{b}, \mathbf{x})\} \quad (25)$$
where $z_{x=0}(\mathbf{b}, \mathbf{x})$ is the displacement at the middle of the

span and $A(\mathbf{b}, \mathbf{x})$ is the net-sectional area of the stiffened plate, $\mathbf{b}=\{ \sigma_y, E\}^{-1}$.

3.3 Constraints

The dimensions of the flange, web and attached plate of the stiffened plate have to satisfy the following constraints:

$$G_1: \ x_1 - \frac{b_p}{C} \sqrt{\frac{\sigma_y}{235}} > 0 \quad (26)$$

$$G_2: \ x_3 - \frac{h_w}{C_w} \sqrt{\frac{\sigma_y}{235}} > 0 \quad (27)$$

$$G_3: \ x_5 - \frac{b_f}{C_f} \sqrt{\frac{\sigma_y}{235}} > 0 \quad (28)$$

$$G_4: \ \sigma_u(\mathbf{b}, \mathbf{x}) - \sigma_{max, \, x=0}(\mathbf{b}, \mathbf{x}) > 0 \quad (29)$$
$$G_5: \ \pi/2 - u^*(\mathbf{b}, \mathbf{x}) > 0 \quad (30)$$

where b_p is the space defined as a distance between the longitudinal stiffeners (see Figure 1 and Figure 2), $C=100$, $C_w=75$, $C_f=12$ (IACS, 2012), $\sigma_{max,x=0}(\mathbf{b}, \mathbf{x})$ is the mean value of the stresses calculated at the middle of the span, $x=0$, of the stiffened plate and $\sigma_u(\mathbf{b}, \mathbf{x})$ is the mean value of the ultimate strength.
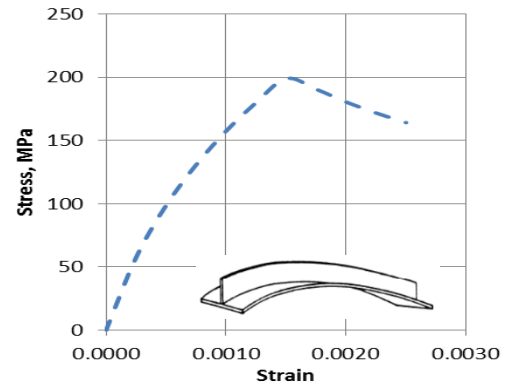

Figure 5 Mean value stress-strain relationship, design solution n° 58.

The type of load subjected to stiffened plate will induce plate buckling since the stiffener is subjected to a tensile load and the attached plate to compressive load. The numerically estimated stress-strain relationship of the design solution n° 58 is presented in Figure 5.

3.4 Pareto Frontier

The Pareto frontier (Komuro et al., 2006) is employed here allowing for the optimization of the two criterion, as they are defined in the present study as the minimum net sectional area and displacement, verifying all trade-offs among the optimal design solutions of the two criterion. Figure 6 shows the minimization of the two objective functions, F_1 (net sectional area) and F_2 (displacement) simultaneously.

The curve in Figure 6 indicates the Pareto optimal

frontier, whereby any improvement with respect to F_1 comes at the expense of F_2. Each design solution, allocated at that frontier, represents unique design solution parameters. The Pareto optimal solution collected here 100 optimal design solutions that are going to be verified with respect to the target reliability in the next section, leading to an additional constraint in the optimization process.
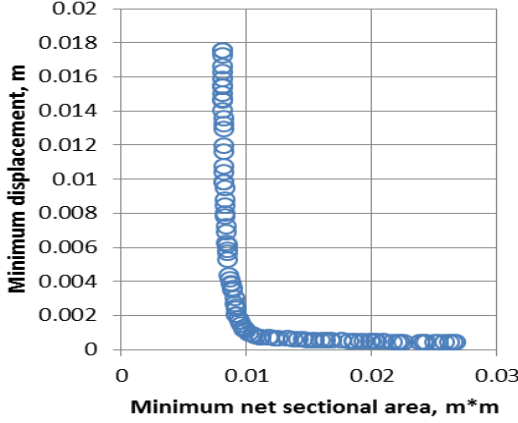

Figure 6 Pareto frontier

The forward finite difference method (Ames, 1977) is used to compute the first derivation of the design variables as defined by the Pareto frontier with respect to the mean of the limit state $E[g(\mathbf{b}, \mathbf{x})]= E[\sigma_u(\mathbf{b}, \mathbf{x})]-E[\sigma_{max,x=0}(\mathbf{b}, \mathbf{x})]$ by making a small perturbation in the corresponding variables while keeping other design variables constant. In this study, a 1% perturbation is assumed in each of the variables. The sensitivity of the design variables is calculated by:

$$\alpha_{xi} = \frac{1}{\sqrt{\sum_{i=1}^{n}\left(\frac{E[g(\mathbf{b},\mathbf{x})]}{\partial x_i}\right)^2}} \frac{\partial E[g(\mathbf{b},\mathbf{x})]}{\partial x_i} \qquad (31)$$

where $\mathbf{x}=\{ x_1, x_2, x_3, x_4, x_5\}^{-1}$ and $\mathbf{b}=\{ \sigma_y, E\}^{-1}$ and are shown in Figure 7.

As can be seen from Figure 7, the most sensitive parameters in defining the design solutions is t_p followed by t_w, t_f, h_w and b_f. However, b_p and l are kept constant and they are not a part of the design solution here.
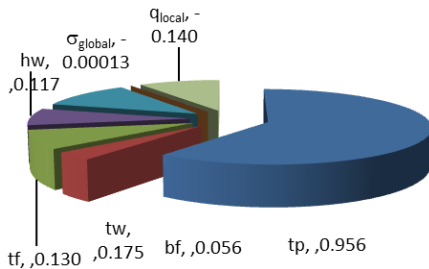

Figure 7 Design variable sensitivities with respect to the limit state stresses, design solution n° 58.

4 RELIABILITY-BASED DESIGN OPTIMIZATION

The reliability analysis is incorporated into the optimization procedure, which is referred to here as a reliability-based design optimization, RBDO. The statistical nature of the constraints and design problems are defined in the objective function and probabilistic constraints. The probabilistic constraint can specify the required reliability target level.

The formation of RBDO is similar to the one of the optimization where the objective limits state function), $g(\mathbf{b}, \mathbf{x})$ is minimized and it is subject to constraints, where $\mathbf{b}$ is the vector of the deterministic design variables and $\mathbf{x}$ is the vector of the random variables.

The limit state function here is defined as:

$$g(\mathbf{b},\mathbf{x}) = \sigma_u(\mathbf{b},\mathbf{x}) - \sigma_{max,x=0}(\mathbf{b},\mathbf{x}) \qquad (32)$$

and the safety index is defined as:

$$\beta_g \geq \beta_{target} \qquad (33)$$

where β_{target} is the required target safety index and, β_g is the safety index of the probabilistic constraints.

The reliability analysis performed here is using the FORM techniques that identify a set of basic random variables, which influence the failure mode or the limit-state under consideration. The limit-state function defines a failure surface when equals to 0, which is in fact an (n-1) dimensional surface in the space of n basic variables. This surface divides the basic variable space in a safe region, where $g(\mathbf{b}, \mathbf{x})>0$ and an unsafe region where $g(\mathbf{b}, \mathbf{x})<0$. The failure probability of a structural component with respect to a single failure mode can formally be written as:

$$P_f = P[g(\mathbf{b},\mathbf{x}) \leq 0] \qquad (34)$$

where P_f denotes the probability of failure. In practical applications. The FORM methods provide a way of evaluating the reliability efficiently with reasonably good accuracy as proposed by Hasofer and Lind (1974), Rackwitz and Filessler (1978), Ditlevsen (1979).

The required safety index is defined here as β_{target}. The Beta index of all feasible design solutions, as defined by the Pareto frontier, is compared to the required target safety index, where $min\{\beta_{target} - \beta_i\}$ is the best reliability based design solution.

Seven deterministic variables are considered here as $b_1 = t_p$, $b_2 = b_f$, $b_3 = t_f$, $b_4 = h_w$, $b_5 = t_w$, $b_6 = \sigma_y$, $b_7 = E$, and ten random variables $x_1 = M_{w,BL,hog}$, $x_2 = P_{w,BL,h}$, $x_3 = M_{sw,BL,h}$, $x_4 = P_{sw,BL,h}$, $x_5 = \sigma_u$, $x_6 = X_u$, $x_7 = X_{p,sw}$, $x_8 = X_{m,sw}$, $x_9 = X_{p,d}$, $x_{10} = X_{m,d}$ are considered here, where $\mathbf{x}=\{M_{w,BL,hog}, P_{w,BL,h}, M_{sw,BL,h}, P_{sw,BL,h}, \sigma_u, X_u, X_{p,sw}, X_{m,sw}, X_{p,d}, X_{m,d}\}^{-1}$ and $\mathbf{b}=\{t_p, b_f, t_f, h_w, t_w, \sigma_y, E\}^{-1}$.

The lateral local load is defined as $q_{local.}=(X_{p,sw} P_{sw,BL,h}+\psi X_{p,w} P_{w,BL,h})b$ and the net-sectional stresses, resulting from the global bending load, is $\sigma_{global}= (X_{m,sw} M_{sw,BL,h} + \psi X_{m,w} M_{w,BL,h}) /W_b$. σ_u is the ultimate stress capacity with a model uncertainty factor X_u, which is

assumed to be described by the Normal probability density function, $N_{x,u}(1.05, 0.1)$.

The model uncertainty factor $X_{m,w}$ accounts for the uncertainties in the wave induced vertical bending moment calculation, where $X_{m,wl}$ accounts for the uncertainties in the linear response calculation and $X_{m,nl}$ for the nonlinear effects. The total uncertainty of the random variable $X_{m,w}$ BL with a mean value and coefficient of variation determined by:

$$E(X_{m,w})=E(X_{m,w,l})E(X_{m,w,nl}) \tag{35}$$
$$Cov(X_{m,w})=\sqrt{[(1+Cov(X_{m,w,l})^2)(1+Cov(X_{m,w,nl})^2)-1]} \tag{36}$$
$$\sigma_{m,w}=Cov(X_{m,w}) E[X_{m,w}] \tag{37}$$

resulting in $X_{m,w}{\sim}N_{x,m,w}(1, 0.1)$ and the model uncertainty factor with respect to the still water load is $X_{m,sw}{\sim}N_{x,m,sw}(1, 0.1)$ and with respect to the local pressure load are modelled by $X_{p,sw}{\sim}N_{p,sw}(1, 0.1)$ and $X_{p,w}{\sim}N_{p,w}(0.95, 0.095)$.

The fraction of time spent in each load condition may be estimated based on the statistical analysis of the operational profile of the tanker ship. The assumed operational profile here is: full load, $p_{FL}=0.4$, ballast load, $p_{BL}=0.4$, partial load, $p_{PL}=0.1$ and harbour load, $p_{HL}=0.1$. The vertical wave-induced bending moment is in sagging in the full loading condition and in hogging in ballast and partial loading conditions. The still water bending moment is in sagging in full loading and in hogging in ballast and partial loading conditions. The ballast loading case is used in the present analysis since it transmits a compressive load to the stiffened plate at the bottom of the ship.

The still water bending moment is fitted to a Normal distribution. The statistical descriptors of the still water bending moment are defined by the regression equations as a function of the length of the ship, L and dead-weight ratio, W= (DWT/Full load) as proposed by Guedes Soares and Moan (1988), Guedes Soares (1990) and the loads are taken as prescribed by the Classification Societies Rules (IACS, 2012).

The statistical descriptors of the still water bending moment in the ballast loading case are $N_{m,sw,h,BL}(192$ MN.m, 73 MN.m) and for the local pressure load, $N_{p,sw,h,BL}(0.044$ MPa, 0.017 MPa). The still water load is in a hogging condition for the ballast load condition.

The stochastic model of the vertical wave-induced bending moment, as proposed by Guedes Soares et al. (1996), is employed here. The distribution of the extreme values of the wave-induced bending moment at a random point of time, over a specified time period, is assumed as a Gumbel distribution, considering that the wave-induced bending moment can be represented as a stationary Gaussian process (short-term analysis), then the vertical wave-induced bending moment, $M_w{}^{CSR}$ as given by CSR, may be modelled as a Weibull distribution with a probability of exceedance of 10^{-8}.

The Gumbel distribution, $G(\alpha_m, \beta_m)$ for the extreme values of the vertical wave-induced bending moment, over the reference period T_r, is derived based on the shape, h and scale, λ factors of the Weibull distribution function, W(q, h) as proposed by Guedes Soares et al.

(1996), where q is the scale factor and h is the shape parameter:

$$\alpha_m = \lambda\left(\ln(n)\right)^h \tag{38}$$
$$\beta_m = \frac{q}{h}\left(\ln(n)\right)^{(1-h)/h} \tag{39}$$

where α_m and β_m are the parameters of the Gumbel distribution, n is the mean number of load cycles, expected over the reference time period T_r, for a given mean value wave period T_w. It is also assumed here that $T_r=1$ year and $T_w=8$ sec. The mean number of the load cycles n_i is calculated as $n_i=p_iT_r/T_w$, when the ship is in different seagoing conditions for i= BL, BL, PL and HL.

The extreme value of the vertical wave-induced bending moment in the ballast loading condition are defined by the Gumbel distribution as $G_{m,w,h,BL}(607$ MN.m, 29 MN.m) and for local pressure load as $G_{p,w,h,BL}(0.013$ MPa, 0.001 MPa) respectively.

The 5% confidence level value of the ultimate stresses, $\sigma_u{}^{5\%}$ is calculated by an algorithm as stipulated by IACS (2012), which is based on an incremental-iterative approach procedure for estimating the elasto-plastic failure of the stiffened plate, σ_u (Garbatov et al., 2016b). Additionally, it is assumed that CoV is 0.08 and the estimated value is fitted to the Log-normal probability density function.

The deterministic variables b_1 to b_5 are defined by the Pareto frontier and $\sigma_y=315$ MPa and E=206 GPa.

The reliability is performed based on FORM and all random variables are considered as non-correlated ones. Applying FORM as a decision tool, the estimated probability of failure needs to be compared to an accepted target level. The target levels depend on different factors as reported by Moan (1998). The target level adapted here is related to failure cause and mode, which may result for a redundant structure in $P_f=10^{-3}$ ($\beta=3.09$) for less serious and $P_f=10^{-4}$ ($\beta=3.71$) for serious consequences of failure values of the acceptable annual probability of failure (DnV, 1992).

5 RESULTS AND DISCUTIONS

The Beta index, as a function of the two objective functions, is presented in Figure 8. The minimum and maximum values of the Beta index of all design solutions at the Pareto frontier are 0.8 and 7.9. The design solution nº 58, $\beta=3.7$ fits all constrains of the two objective functions and the required safety target level, as defined to be here, $\beta_{target}=3.7$.

Figure 8 shows that the maximum Beta index is located in the lower right hand side where the maximum net sectional area and minimum displacement are located and the minimum Beta is located in the upper left side, where the maximum displacement and minimum net sectional area are placed. The size of the bubble represents the value of the Beta index.
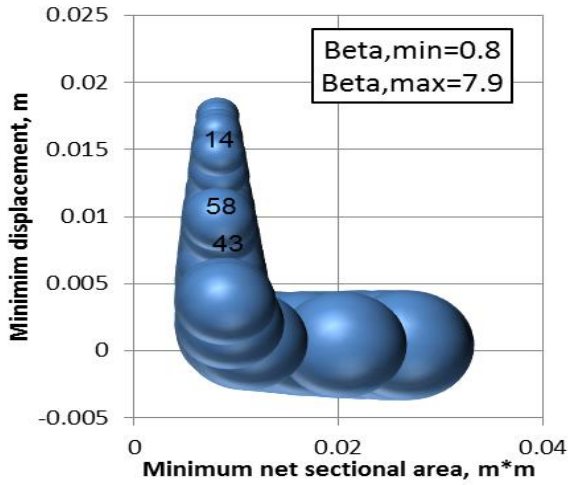
Figure 8 Beta index as a function of the net sectional area and displacement at the Pareto frontier

Table 1 Topology of stiffened plate

nº	β	t_p, m	b_f, m	t_f, m	h_w, m	t_w, m
14	2.0	0.009	0.038	0.004	0.146	0.004
58	3.7	0.009	0.044	0.006	0.174	0.005
43	5.0	0.009	0.058	0.008	0.201	0.006

Figure 9 shows the Beta index of the design solutions as a function of the net sectional area and displacement. The topology of the stiffened plate for the design solution nº 14 (β=2.0), nº 58 (β=3.7) and nº 43 (β=5.0) are presented in Table 1. The design values of the random variables of the design solution nº 58 are presented in Table 2.
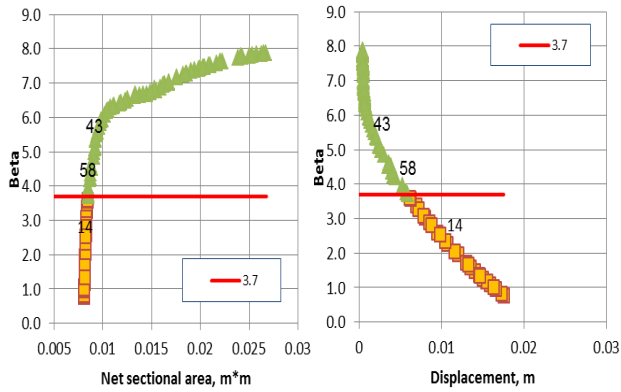

Figure 9 Beta index as a function of the net sectional area (left) and displacement (right)

The importance of the contribution of each random variable to the limit state function $g^*(\mathbf{b}, \mathbf{x})$ at the design point can be assessed by the sensitivity factors, which are determined as:

$$\alpha_{xi} = \frac{1}{\sqrt{\sum_{i=1}^{\infty}\left(\frac{\partial g^*(\mathbf{b},\mathbf{x})}{\partial x_i}\right)^2}} \frac{\partial g^*(\mathbf{b},\mathbf{x})}{\partial x_i} \quad (40)$$

Table 2 Design values of random variables, design solution nº 58, β=3.7

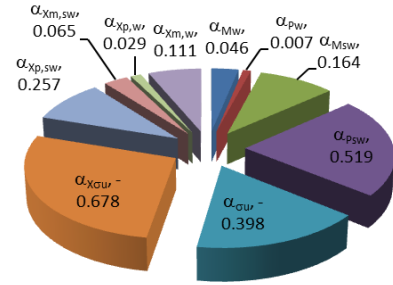| $M^*_{w,h,BL}$, MNm	$P^*_{w,h,BL}$, MPa	$M^*_{sw,h,BL}$, MNm	$P^*_{sw,h,BL}$, MPa	σ^*_u, MPa
619.107	0.013	295.329	0.062	272.043
$X^*_{m,w}$	$X^*_{p,w}$	$X^*_{m,sw}$	$X^*_{p,sw}$	$^*X_u$
1.103	0.956	1.054	1.036	0.302

Figure 10 Sensitivity indexes of the random variables, nº 58, β=3.7

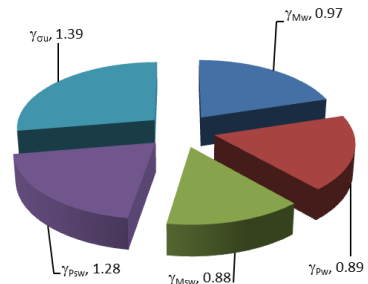

Figure 11 Partial safety factors, nº 58, β=3.7

A positive sensitivity indicates that with an increase in the variable results in an increase in the limit state function, which will reduce the probability of failure and contributes to an increase in reliability.

The most important random variable in the present reliability analysis is $X_{\sigma,u}$, followed by P_{sw}, σ_u and $X_{p,sw}$. The lateral load and axial global stresses and associated uncertainty modelling factors contribute negatively to the structural capacity and reliability (see Figure 10).

Partial safety factors can be estimated based on the characteristic values of σ_u^c, M_{sw}^{CSR}, M_w^{CSR}, P_{sw}^{CSR}, P_w^{CSR} calculated at 5% confidence level of the original probability density function and as provided by CSR respectively. The design values of all parameters involved in the limit state functions are M^*_w, P^*_w, M^*_{sw}, P^*_{sw}, σ^*_u, $X^*_{\sigma,u}$, $X^*_{p,sw}$, $X^*_{m,sw}$, $X^*_{p,w}$, $X^*_{m,w}$ are respecting the Beta reliability index, which in the case of the design solution nº 58 is β=3.7 and the partial safety factors are defined as:

$$\gamma_{\sigma,u} = \frac{\sigma_u^c}{X^*_{\sigma,u}\sigma^*_u}, \ \gamma_{m,sw} = \frac{X^*_{m,sw}M^*_{sw}}{M_{sw}^{CSR}}, \ \gamma_{m,w} = \frac{X^*_{m,w}M^*_w}{M_w^{CSR}} \quad (41)$$

$$\gamma_{p,sw} = \frac{X^*_{p,sw}P^*_{sw}}{P_{sw}^{CSR}}, \ \gamma_{p,w} = \frac{X^*_{p,w}P^*_w}{P_w^{CSR}} \quad (42)$$

The resulting partial safety factors can be used in the preliminary design by satisfying the following design criterion:

$$\frac{\sigma_u}{\gamma_{\sigma,u}} \geq \sigma_{max,x=0}\left(q_{local}, \sigma_{global}\right) \quad (43)$$

where:

$$q_{local} = \left(\gamma_{psw} P_{sw}^{CSR} + \gamma_{pw} P_w^{CSR} \right) b_p \qquad (44)$$

$$\sigma_{global} = \left(\gamma_{msw} M_{sw}^{CSR} + \gamma_{mw} M_w^{CSR} \right) / W_{bottom\ ship} \qquad (45)$$

The estimated partial safety factors for the analysed stiffened plate here are presented in Figure 11.

If the cost of manufacturing needs to be accounted for, then the risk of losing the stiffened plate as an integral part of the ship hull may be calculated as:

$$\text{Risk} = (P_f)(C) \qquad (46)$$

where $P_f = 1 - R$, is the probability of failure, $R = \Phi^{-1}(-\beta)$ is the reliability and C is the consequences measured by the cost of the material and construction are assumed here as 2500USD/ton. The estimated risk as a function of displacement is shown in Figure 12.
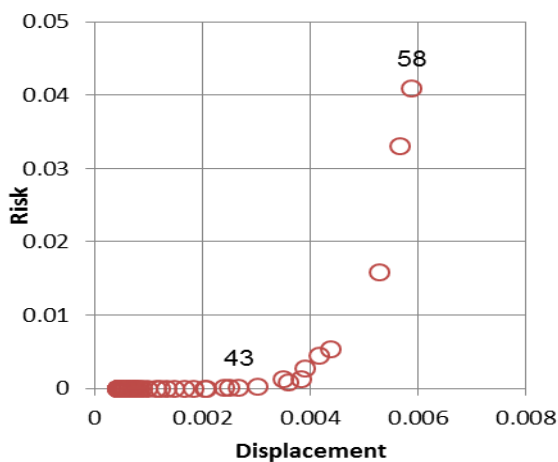

Figure 12 Risk as a function of displacement

The already discussed design solutions 14, 58 and 43 take risk values of 7.7, 0.04 and 0.00013 respectively, resulting from the cost values of 384.2, 397.2 and 425.7 USD and probability of failure of 0.02, 0.0001 and 3E-07.

6 CONCLUSION

The objective of this work was to perform a multi objective nonlinear structural optimization of a stiffened plate subjected to combined stochastic compressive loads accounting for the ultimate strength and reliability based constraints in the design. The solution of a dual objective structural response, in minimizing the weight and structural displacement, was considered. The Pareto frontier solution was used to define the feasible surface solution of the design variables.

The reliability index, which defines the shortest distance from the origin to the limit-state boundary, was employed to identify the topology of the stiffened plate as a part of the Pareto frontier solution. The sensitivities of the design and random variables were analysed demonstrating the most influencing ones. Partial safety factors were derived that can be used in the conception

design, avoiding a complex structural analysis, which is one of the objective of the project SHIPLYS.

The presented methodology is flexible and demonstrated a good capacity to be used in structural design of complex systems.

ACKNOWLEDGEMENTS

REFERENCES

Ames, W. F. 1977. *Numerical Methods for Partial Differential Equations,* New York, Academic Press.

Deb, K., Pratap, A., Agrawal, S. & Meyarivan, T. 2002. A Fast and Elitist Multi-objective Genetic Algorithm: NSGA-II. *IEEE Transactions on Evolutionary Computation,* 6**,** 182-197.

Ditlevsen, O. 1979. Generalised second moment reliability index. *Journal of Structural Mechanics,* 7**,** 435-451.

Dnv 1992. Structural Reliability Analysis of Marine Structures. *Classification notes No 30.6.* Hovik: DnV.

Garbatov, Y. & Guedes Soares, C. 2008. Reliability of aged ship structures. *In:* Paik, J. & Melchers, R. (eds.) *Condition Assessment of Aged Structures.* Cambridge, UK: Woodhead Publishing Limited, 253-286.

Garbatov, Y. & Guedes Soares, C. 2011. Fatigue reliability assessment of welded joints of very fast ferry subjected to combined load. *International Journal of Maritime Engineering (RINA Transactions Part A),* 153**,** 231-241.

Garbatov, Y., Guedes Soares, C., Parunov, J. & Kodvanj, J. 2014. Tensile Strength Assessment of Corroded Small Scale Specimens. *Corrosion Science,* 85**,** 296–303.

Garbatov, Y., Parunov, J., Kodvanj, J., Saad-Eldeen, S. & Guedes Soares, C. 2016a. Experimental assessment of tensile strength of corroded steel specimens subjected to sandblast and sandpaper cleaning. *Marine Structures,* 49**,** 18-30.

Garbatov, Y., Tekgoz, M. & Guedes Soares, C. 2011. Uncertainty assessment of the ultimate strength of a stiffened panel. *In:* Guedes Soares, C. & Fricke, W. (eds.) *Advances in Marine Structures.* London, UK: Taylor & Francis Group, 659-668.

Garbatov, Y., Tekgoz, M. & Guedes Soares, C. 2016b. Experimental and numerical strength assessment of stiffened plates subjected to severe non-uniform corrosion degradation and compressive load. *Ships and Offshore Structures***,** DOI 10.1080/17445302.2016.1173807.

Georgiev, P. & Naydenov, L. 2015. Probabilistic limit state analysis of ship survival index. *In:* Guedes Soares, C., Dejhalla & Pavletic (eds.) *Towards Green Marine Technology and Transport.* London: Taylor & Francis Group, 419-425.

Guedes Soares, C. 1990. Stochastic Modelling of Maximum Still-Water Load Effects in Ship Structures. *Journal of Ship Research,* 34**,** 199-205.

Guedes Soares, C., Dogliani, M., Ostergaard, C., Parmentier, G. & Pedersen, P. T. 1996. Reliability Based Ship Structural Design. *Transactions of the Society of Naval Architects and Marine Engineers (SNAME),* 104**,** 359-389.

Guedes Soares, C. & Moan, T. 1988. Statistical Analysis of Still-Water Load. Effects in Ship Structures. *SNAME Transactions,* 96**,** 129-156.

Hasofer, A. M. & Lind, N. C. 1974. An exact and invariant first-order reliability format. *Journal of Engineering Mechanics Division,* 100**,** 111-121.

Iacs 2012. Common Structure Rules for Double Hull Oil Tankers, Consolidated version, July 2012.

Komuro, R., Ford, E. D. & Reynolds, J. 2006. The use of multi-criteria assessment in developing a process model. *Ecological Modelling,* 197**,** 320-330.

Moan, T. 1998. Target levels for structural reliability and risk analyses of offshore structures. *In:* Soares, G. (ed.) *Risk and reliability in marine technology.* Rotterdam: A.A. Balkema.

Rackwitz, R. & Fiessler, B. Structural Reliability Under Combined Random Load Sequences. Computers and Structures, 1978 1978. 489-494.

Rackwitz, R. & Filessler, B. 1978. Structural Reliability under Combined Random Load Sequences. *Computers & Structures,* 9**,** 489-494.

Shimansky 1956. *Shipbuilding mechanics,* Leningrad, Sudprogiz.

Silva, J. E., Garbatov, Y. & Guedes Soares, C. 2013. Ultimate Strength Assessment of Rectangular Steel Plates Subjected to a Random Non-Uniform Corrosion Degradation. *Engineering Structures,* 52**,** 295-305.

Tekgoz, M., Garbatov, Y. & Guedes Soares, C. 2012. Ultimate strength assessment accounting for the effect of finite element modelling. *In:* Guedes Soares, C., Garbatov, Y., Sutulo, S. & Santos, T. (eds.) *Maritime Engineering and Technology.* London, UK: Taylor & Francis Group, 353-362.

Tekgoz, M., Garbatov, Y. & Guedes Soares, C. 2013a. Finite element modelling of the ultimate strength of stiffened plates with residual stresses. *In:* Guedes Soares, C. & Romanoff, J. (eds.) *Analysis and Design of Marine Structures.* London, UK: Taylor & Francis Group, 309-317.

Tekgoz, M., Garbatov, Y. & Guedes Soares, C. Ultimate strength assessment of a stiffened plate accounting for welding sequences. *In:* Chang-Sup Lee, S.-H. V., ed. Proceedings of the 11th International Symposium on Practical Design of Ships and other Floating Structures (PRADS 2013), 2013b Changwon City, Korea. CECO, 1089-1095.

Tekgoz, M., Garbatov, Y. & Guedes Soares, C. 2014. Ultimate strength of a plate accounting for the effect of shakedown and corrosion degradation. *In:* Guedes Soares, C. & Pena, F. (eds.) *Developments in Maritime Transportation and Exploitation of Sea Resources.* London, UK: Taylor & Francis Group, 395-403.

Timoshenko, S. P. & Gere, J. M. 1986. *Theory of Elastic Stability*, McGraw-Hill Book Company.

Wong, J. Y. Q., Sharma, S. & Rangaiah, G. P. 2015. Design of Shell-and-Tube Heat Exchangers for Multiple Objectives using Elitist Non-dominated Sorting Genetic Algorithm with Termination Criteria.